Ridged Waveguides with Inhomogeneous Dielectric-Slab Loading

GOTTFRIED MAGERL, MEMBER, IEEE

Abstract—**The dispersion equation of the ridged waveguide with inhomogeneous dielectric-slab loading is derived. Numerical results for the cutoff frequencies of the three lowest order TE_{m0} modes are given which substantiate the feasibility of the modal expansion and field-matching technique employed. For a Teflon-slab loaded ridged waveguide, a 40-percent decrease of dominant-mode cutoff frequency, simultaneously providing 20-percent enhanced TE_{20}-mode separation compared to an empty ridged waveguide, is demonstrated.**

I. Introduction

EMPTY RIDGED waveguides are in wide use because of their low cutoff frequency and considerable bandwidth of the dominant mode. Usually the cutoff frequencies are calculated employing a transverse resonance method [1]–[5] based on an equivalent circuit of two cascaded transmission lines of different wave impedances. The field distortions caused by the abrupt change of the waveguide's height are accounted for by a shunt capacitance between the connecting terminals of the transmission lines in the equivalent circuit. Values for this capacitance can be found in [6] and [7].

The transverse resonance method, however, is not immediately applicable to inhomogeneously dielectrically loaded ridged waveguides, due to the lack of values for the fringing capacitances. Other powerful methods seemingly capable for the solution of this problem are failing too; conformal mapping fails for a change of media at the waveguide's step [8], and the use of the theory of singular integral equations [9]–[11] is restricted to integrally related step ratios [8].

As ridged waveguides with inhomogeneous dielectric loading seemed promising for obtaining still greater bandwidth than ordinary ridged guides, a general solution of this propagation problem which is presented in this paper was sought. The technique employed is a refinement and combination of modal expansion and transverse field matching [7]–[12]. Numerical results for the cutoff frequencies of the three lowest order TE_{m0} modes are calculated to establish the feasibility of the method. A drastic decrease of the cutoff frequency of the dominant mode, simultaneously providing substantially enhanced TE_{20}-mode separation in comparison with empty ridged waveguides, is demonstrated.

Manuscript received May 16, 1977; revised September 7, 1977. This work was supported by the Fonds zur Förderung der wissenschaftlichen Forschung, Vienna, Austria.

The author is with the Institut für Hochfrequenztechnik of the Technical University of Vienna, A-1040 Vienna, Austria.

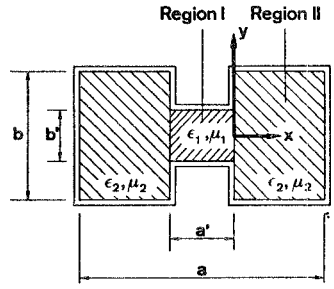

Fig. 1. Cross section of ridged waveguide with inhomogeneous dielectric-slab loading.

II. Field Description

In this section the dispersion equation for TE_{m0} modes will be derived. The electromagnetic (EM) field components of the TE_{m0} modes in the slab-loaded ridged waveguide shown in Fig. 1 can be described by a linear combination of the undisturbed TE_{m0}-mode pattern of a slab-loaded rectangular waveguide and of higher order TE modes. This concept was implemented for both regions I and II of the cross section (Fig. 1). Reflection of the higher order modes from the waveguide walls, the reason for "proximity effects" [2], is accounted for by choosing hyperbolic functions to describe the x dependence of these modes.

For region I of the cross section ($-a' \leqslant x \leqslant 0$ in Fig. 1), the field components can be written as[1]

$$E_{x1} = \omega\mu_1 H_{y1}/k_z = E_1 \exp(-jk_z z) \cdot \sum_n (k_{y1} C_{n1}/\Gamma_{n1}) R_n \frac{\sinh}{\cosh}(\Gamma_{n1}\xi_1) \sin(k_{y1} y)$$

$$E_{y1} = -\omega\mu_1 H_{x1}/k_z = E_1 \exp(-jk_z z)\left[\frac{\cos}{\sin}(k_{x1}\xi_1) + \sum_n C_{n1} R_n \frac{\cosh}{\sinh}(\Gamma_{n1}\xi_1) \cos(k_{y1} y)\right]$$

$$E_{z1} = 0$$

$$H_{z1} = (1/j\omega\mu_1) E_1 \exp(-jk_z z)\left[k_{x1} \frac{\sin}{-\cos}(k_{x1}\xi_1) + k_{x1}^2 \sum_n (C_{n1}/\Gamma_{n1}) R_n \frac{\sinh}{\cosh}(\Gamma_{n1}\xi_1) \cos(k_{y1} y)\right]. \quad (1)$$

[1]In this notation, the symmetric modes (m odd) are described by the upper symbols for the trigonometric and hyperbolic functions, whereas the lower symbols apply to the antisymmetric modes (m even).

0018-9480/78/0600-0413$00.75

The components of the EM field in region II of the cross section $(0 \leqslant x \leqslant (a-a')/2)$ are described by

$$E_{x2} = \omega\mu_2 H_{y2}/k_z = -E_2 \exp(-jk_z z) \cdot \sum_n (k_{y2} C_{n2}/\Gamma_{n2}) T_n \cosh(\Gamma_{n2}\xi_2) \sin(k_{y2} y)$$

$$E_{y2} = -\omega\mu_2 H_{x2}/k_z = E_2 \exp(-jk_z z)\left[\sin(k_{x2}\xi_2) + \sum_n C_{n2} T_n \sinh(\Gamma_{n2}\xi_2) \cos(k_{y2} y)\right]$$

$$E_{z2} = 0$$

$$H_{z2} = (1/j\omega\mu_2) E_2 \exp(-jk_z z)\left[k_{x2} \cos(k_{x2}\xi_2) - k_{x2}^2 \sum_n (C_{n2}/\Gamma_{n2}) T_n \cosh(\Gamma_{n2}\xi_2) \cos(k_{y2} y)\right] \quad (2)$$

where ω is the angular frequency, and ϵ_i and μ_i are the permittivity and the permeability of the inner $(i=1)$ and the outer $(i=2)$ parts of the cross section, respectively. The quantities E_i stand for the amplitudes of the complete mode pattern, whereas the R_n's and T_n's are the amplitudes of the higher order TE modes. The ξ_i's and the C_{ni}'s are abbreviations for

$$\xi_1 = x + a'/2$$
$$\xi_2 = -x + (a-a')/2 \quad \text{and} \quad (3)$$
$$C_{n1} = \begin{matrix}\cos \\ \sin\end{matrix}(k_{x1}a'/2) \Big/ \begin{matrix}\cosh \\ \sinh\end{matrix}(\Gamma_{n1}a'/2)$$
$$C_{n2} = \frac{b \sin\left[k_{x2}(a-a')/2\right]}{b' \sinh\left[\Gamma_{n2}(a-a')/2\right]}. \quad (4)$$

The symbol k_z denotes the (real) propagation constant of the complete mode; k_{xi} are the wavenumbers in the x direction of the undisturbed parts of the mode pattern, whereas Γ_{ni} and k_{yi} are the wavenumbers of the higher order TE modes in the x and y direction, respectively.

Introducing the field components (1) and (2) into Maxwell's equations yields the separation conditions

$$k_{xi}^2 = \omega^2\epsilon_i\mu_i - k_z^2$$
$$\Gamma_{ni}^2 = k_{yi}^2 + k_z^2 - \omega^2\epsilon_i\mu_i, \qquad i = 1,2. \quad (5)$$

Whenever $k_z^2 > \omega^2\epsilon_2\mu_2$ applies, the wavenumber k_{x2} has to be replaced by $j|k_{x2}|$, giving rise to an aperiodic field distribution in (2).

Now we match the inner and outer tangential field components at $x=0$; the cosines $\cos(k_{yi}y)$ appear in the series terms of the matching equations. Since the wavenumbers k_{yi} are given by

$$k_{y1} = 2n\pi/b'$$
$$k_{y2} = 2n\pi/b \quad (6)$$

where n is an integer, and b' and b are the heights of the inner and outer parts of the waveguide's cross section according to Fig. 1, the outer fields may be interpreted as a Fourier expansion of the inner fields at the $x=0$ interface [7]. Evaluation of the lowest order Fourier coefficient (corresponding to the undisturbed part of the electric field) leads to

$$E_2 = \frac{b' \begin{matrix}\cos \\ \sin\end{matrix}(k_{x1}a'/2)}{b \sin\left[k_{x2}(a-a')/2\right]} E_1. \quad (7)$$

Introducing this equation into the EM field components (1) and (2), the remaining Fourier coefficients of the electric field can now be calculated to get

$$T_n = 2\alpha \operatorname{sinc}(n\pi\alpha) + \alpha \sum_j R_j \{\operatorname{sinc}[(j+n\alpha)\pi] + \operatorname{sinc}[(j-n\alpha)\pi]\} \quad (8)$$

where the definitions $\alpha = b'/b$ and $\operatorname{sinc}(x) = \sin(x)/x$ have been used. The next step is to determine the higher order mode amplitudes by applying a corresponding Fourier expansion to the magnetic field components at $x=0$

$$R_j = -(\mu_1 k_{x2}^2/\mu_2 k_{x1}^2)\Gamma_{j1} \begin{matrix}\coth \\ \tanh\end{matrix}(\Gamma_{j1}a'/2) \cdot \sum_k (T_k/\Gamma_{k2}) \coth\left[\Gamma_{k2}(a-a')/2\right] \cdot \{\operatorname{sinc}[(j+k\alpha)\pi] + \operatorname{sinc}[(j-k\alpha)\pi]\}. \quad (9)$$

Introducing (9) into (8) yields

$$T_n = 2\alpha \operatorname{sinc}(n\pi\alpha) - (\mu_1 k_{x2}^2/\mu_2 k_{x1}^2) \sum_j \Gamma_{j1} \begin{matrix}\coth \\ \tanh\end{matrix}(\Gamma_{j1}a'/2) \cdot \{\operatorname{sinc}[(j+n\alpha)\pi] + \operatorname{sinc}[(j-n\alpha)\pi]\} \cdot \sum_k (T_k/\Gamma_{k2}) \coth\left[\Gamma_{k2}(a-a')/2\right] \cdot \{\operatorname{sinc}[(j+k\alpha)\pi] + \operatorname{sinc}[(j-k\alpha)\pi]\}. \quad (10)$$

Equation (10) is well suited for an iterative evaluation of the T_n's. Starting with a set of $T_{k,\,\text{old}} = 2\alpha \operatorname{sinc}(k\pi\alpha)$, a new set of T_n can be calculated and reinserted into (10).

Finally, we derive an expression corresponding to (7) for the undisturbed part of the magnetic field, both for m odd

$$(\mu_2 k_{x1}/\mu_1 k_{x2}) \tan(k_{x1}a'/2) - \alpha \cot\left[k_{x2}(a-a')/2\right] + k_{x2} \sum_n (T_n/\Gamma_{n2}) \coth\left[\Gamma_{n2}(a-a')/2\right] \operatorname{sinc}(n\pi\alpha) = 0 \quad (11a)$$

and for m even

$$(\mu_2 k_{x1}/\mu_1 k_{x2}) \cot(k_{x1}a'/2) + \alpha \cot\left[k_{x2}(a-a')/2\right] - k_{x2} \sum_n (T_n/\Gamma_{n2}) \coth\left[\Gamma_{n2}(a-a')/2\right] \operatorname{sinc}(n\pi\alpha) = 0. \quad (11b)$$

Equations (11) may be interpreted as dispersion equations and have to be solved simultaneously with (5), (6), and (10) for allowed sets of propagation constants and wavenumbers at a given frequency.

III. Cutoff Frequencies—Numerical Results

Using the results of Section II, the cutoff frequencies of the three lowest order TE_{m0} modes were calculated by setting $k_z = 0$ and solving (5), (6), (10), and (11). Since the TE_{m0} modes will *not* be the first higher modes in every case, a brief discussion of moding effects is appropriate. In the limit of the dielectric-slab loaded waveguide with an aspect ratio of $b/a = 0.5$, the distorted TM_{11} mode was shown to restrict the bandwidth close to the empty-waveguide value of 2 [13]. However, ridges of even modest depth protruding into the waveguide will short circuit the E_y component of the distorted TM_{11} mode. In this case, the usable bandwidth will be limited by the distorted TE_{01} mode which was found to be the first higher order mode in the empty ridged waveguide [10]. The cutoff wavelength λ_c of this mode is mainly determined by the waveguide height b according to $\lambda_c \approx 2b$. Thus propagation of the distorted TE_{01} mode (and of the distorted TM_{11} mode, too) can be deferred by reducing the waveguide height, and the TE_{20} will be the first higher order mode to limit the usable bandwidth. Whenever a reduction of the waveguide height is undesirable, a mode filter is conceivable; thin metallic fins protruding horizontally at $y = 0$ into region II of the waveguide's cross section will short-circuit any x- and z-electric field components, thus suppressing both the distorted TM_{11} and TE_{01}. The TE_{m0} modes, of course, will not be affected by this mode filter. Therefore, and because a complete modal analysis was not intended, we restricted ourselves to the calculation of the TE_{m0}-cutoff frequencies. This proceeding facilitates direct comparison of our results with [4].

For the numerical analysis, let the ridged waveguide have an aspect ratio of $b/a = 0.5$, and let a Teflon slab ($\epsilon_{r1} = 2.05$) of cross-sectional dimensions a' and b' be placed inside the gap between the ridges, whereas the outer parts of the waveguide's cross section remain empty ($\epsilon_{r2} = 1$). For the computation, the gap width a' ($0 < a' < a$) and the height of the gap b' ($0.1b \leq b' \leq b$) served as parameters.

Fig. 2(a) shows the cutoff wavelength λ_{c10} of the dominant TE_{10} mode normalized to the waveguide broad dimension. Comparison of the graphs of Fig. 2(a) with the results for empty ridged waveguide [4] shows a 40-percent increase in cutoff wavelength. However, the cutoff wavelength of the next TE_{m0} mode, the TE_{20},[2] is not increased by the same amount. Therefore, the dielectric loading increases the TE_{20}-mode separation by about 20 percent (Fig. 2(b)). It should be mentioned that the general shape of Hopfer's graphs [4] is not affected by the slab loading. The starting points of all graphs at $a' = 0$, representing a fin-line structure, are independent of ϵ_{r1} and are therefore identical with those given in [4]. Furthermore, the maximum dominant-mode cutoff wavelength still occurs at $a' \doteq 0.5a$ (Fig. 2(a)). The maximums of the TE_{20}-mode separation graphs (Fig. 2(b)), however, are shifted to lower values of a'; optimum bandwidth with regard to TE_{20} occurs at $a' = 0.23a$. Whenever propagation of the TE_{20} mode is suppressed due to H_{10}-mode excitation or to the use of mode filters, the dominant-mode bandwidth, now limited by the TE_{30} mode, will be somewhat higher. However, maximum bandwidth with respect to TE_{30} is achieved for $a' \doteq 0.4a$ compared to $a' \doteq 0.5a$ in the empty-guide case [1].

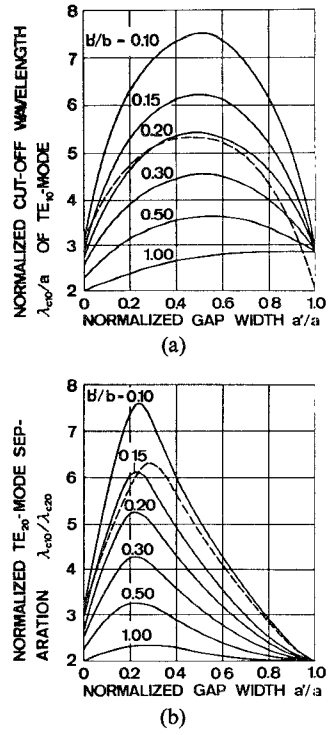

Fig. 2. Gap-width dependence of (a) cutoff wavelength λ_{c10} of the dominant TE_{10} mode normalized to the waveguide broad dimension a, and of (b) TE_{20}-mode separation $\lambda_{c10}/\lambda_{c20}$. The results for a Teflon-slab loaded ridged waveguide ($\epsilon_{r1} = 2.05$, $\epsilon_{r2} = 1$) are represented by solid lines, whereas the dashed curves show Hopfer's graphs [4] for the empty ridged guide ($b'/b = 0.1$).

An increase of the dielectric constant ϵ_{r1} boosts the cutoff wavelength of the dominant mode. Optimum values of this wavelength occur at $a' \doteq 0.5a$ independently of ϵ_{r1} and are shown in Fig. 3(a). Even more important, the TE_{20}-mode separation can be increased, too, which is illustrated in Fig. 3(b). Optimum ridge width a' is reduced from $a' \doteq 0.27a$ for the empty guide to $a' \doteq 0.14a$ for one loaded with an alumina slab ($\epsilon_{r1} = 10$). Consequently, for a given dielectric material, one has to tailor the guide either for low cutoff frequency ($a' \doteq 0.5a$) or for optimum TE_{20}-mode separation ($0.14a \leq a' \leq 0.27a$, depending upon ϵ_{r1}). For optimum results in either case, the gap height b' should be chosen as small as dielectric breakdown permits. We want to emphasize, however, that even a modest ridge of, say, $b' \doteq 0.5b$ will be superior to the dielectric-slab loaded waveguide ($b' = b$) with respect to low cutoff frequency and TE_{20}-mode separation.

IV. Verification of Computational Method

Computational ability and numerical accuracy of the modal expansion and field-matching technique presented

[2]The cutoff frequency of the TE_{30} mode was calculated to be somewhat higher than that of the TE_{20} in all cases.

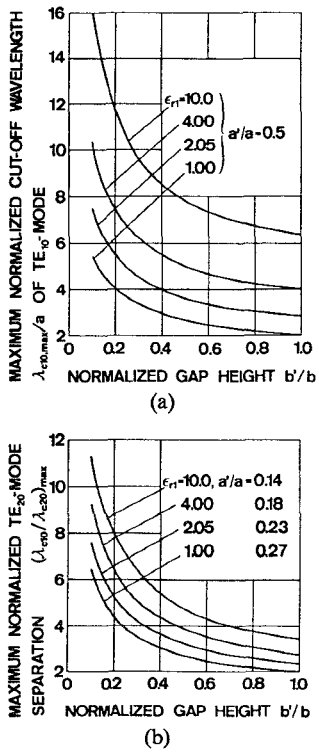

Fig. 3. Gap-height dependence of (a) maximum TE_{10}-cutoff wavelength $\lambda_{c10,\,max}$ normalized to the waveguide broad dimension a, and of (b) maximum TE_{20}-mode separation $(\lambda_{c10}/\lambda_{c20})_{max}$. The permittivity ϵ_{r1} serves as parameter, $\epsilon_{r2}=1$. Note that maximum TE_{10}-cutoff wavelength occurs at $a'/a=0.5$ independent of ϵ_{r1}, whereas maximum TE_{20}-mode separation is achieved for $a'/a=0.14\cdots0.27$, depending on ϵ_{r1}.

here was tested by evaluating the TE_{m0}-cutoff frequencies for several well-known special cases. As a first check, the cutoff frequencies of the homogeneously filled conventional rectangular waveguide were exactly obtained by approaching the limit $a'=a$ and $b'=b$. Next, the corresponding values for the dielectric-slab loaded waveguide were computed by setting $a'\neq a$ and $b'=b$. In this case, too, results identical to previous calculations [14] were obtained. Finally, the cutoff frequencies of the dominant mode of the empty ridged waveguide were computed depending upon $a'\neq a$ and $b'\neq b$ by choosing $\epsilon_{r1}=1$. Comparison of the values obtained by our method with values previously tabulated in [5] showed a consistency to within ± 0.02 percent by employing only five higher order modes, the amplitudes of which were computed in six iterative steps according to (10). Of course, for the dielectric-slab loaded ridged waveguide, such checking opportunities do not exist. Still, for both degenerate cases—the fin-line structure ($a'=0$) and the uniformly filled waveguide ($a'=a$)—the cutoff frequencies approached the well-known values [4] independent of ϵ_{r1}. It follows that the method presented here gives reliable results, even with the consideration of as few as five higher order modes.

V. Conclusions

The dispersion relation of the TE_{m0} modes in the inhomogeneously dielectric-slab loaded ridged waveguide was derived for the first time. Numerical results for this guide substantiated the expectation of prominent differences to the empty ridged waveguide: 1) enhancement of cutoff wavelength, and 2) increase of TE_{20}-mode separation. Also, the ridged guide presented here was shown to be superior to the slab-loaded rectangular waveguide praised as a high-bandwidth device in [15]. Moreover, our approach should prove useful for the investigation of the step discontinuity of the parallel plate line with simultaneous change of media. Such lines were recently proposed as equivalent models for the calculation of fringing field effects in edge-guided wave devices [16].

Acknowledgment

The author would like to express his sincere gratitude to H. Krammer for many stimulating discussions and to E. Bonek for valuable comments during the preparation of the manuscript.

References

[1] S. B. Cohn, "Properties of ridge wave guide," *Proc. IRE*, vol. 35, pp. 783–788, Aug. 1947.
[2] T. G. Mihran, "Closed- and open-ridge waveguide," *Proc. IRE*, vol. 37, pp. 640–644, June 1949.
[3] H. -G. Unger, "Die Berechnung von Steghohlleitern," *Arch. Elek. Ubertragung*, vol. 9, pp. 157–161, Apr. 1955.
[4] S. Hopfer, "The design of ridge waveguides," *IRE Trans. Microwave Theory Tech.*, vol. MTT-3, pp. 20–29, Oct. 1955.
[5] J. R. Pyle, "The cutoff wavelength of the TE_{10} mode in ridged rectangular waveguide of any aspect ratio," *IEEE Trans. Microwave Theory Tech.*, vol. MTT-14, pp. 175–183, Apr. 1966.
[6] N. Marcuvitz, *Waveguide Handbook*. New York: McGraw-Hill, 1951.
[7] J. R. Whinnery and H. W. Jamieson, "Equivalent circuits for discontinuities in transmission lines," *Proc. IRE*, vol. 32, pp. 98–114, Feb. 1944.
[8] J. P. Montgomery and L. Lewin, "Note on an E-plane waveguide step with simultaneous change of media," *IEEE Trans. Microwave Theory Tech.*, vol. MTT-20, pp. 763–764, Nov. 1972.
[9] L. Lewin, "On the resolution of a class of waveguide discontinuity problems by the use of singular integral equations," *IRE Trans. Microwave Theory Tech.*, vol. MTT-9, pp. 321–332, July 1961.
[10] J. P. Montgomery, "On the complete eigenvalue solution of ridged waveguide," *IEEE Trans. Microwave Theory Tech.*, vol. MTT-19, pp. 547–555, June 1971.
[11] L. Lewin, *Theory of Waveguides*. London, England: Newnes–Butterworths, 1975.
[12] W. J. Getsinger, "Ridge waveguide field description and application to directional couplers," *IRE Trans. Microwave Theory Tech.*, vol. MTT-10, pp. 41–50, Jan. 1962.
[13] F. Gardiol, "Higher-order modes in dielectrically loaded rectangular waveguides," *IEEE Trans. Microwave Theory Tech.*, vol. MTT-16, pp. 919–924, Nov. 1968.
[14] E. Bonek and G. Magerl, "Propagation characteristics of dielectrically loaded rectangular waveguides for laser beam modulators," *Arch. Elek. Ubertragung*, vol. 28, pp. 499–506, Dec. 1974.
[15] T. K. Findakly and H. M. Haskal, "On the design of dielectric loaded waveguides," *IEEE Trans. Microwave Theory Tech.*, vol. MTT-24, pp. 39–43, Jan. 1976.
[16] P. DeSantis, "Fringing field effects in edge-guided wave devices," *IEEE Trans. Microwave Theory Tech.*, vol. MTT-24, pp. 409–415, July 1976.